Cosmogenic ^{3}He dating of olivine with tightly retained mantle ^{3}He, Volcano Mountain, Yukon

Jessica M. Mueller[1], Jeff D. Bond[2], Kenneth A. Farley[1], Brent C. Ward[3]
[1]Division of Geological & Planetary Sciences, California Institute of Technology, Pasadena, 91125, USA
[2]Yukon Geological Survey, Yukon, Y1A 2C6, Canada
[3]Simon Fraser University, Burnaby, V5A 1S6, Canada

Correspondence to: Jessica M. Mueller (jessica@caltech.edu)

Abstract. We present a step-heat method for isolating cosmogenic ^{3}He (^{3}He$_c$) from mantle He in olivine xenocrysts to date the eruption of four of the morphologically youngest nephelinite lava flows from Volcano Mountain (VM), the youngest cone in the Fort Selkirk volcanic field in Yukon, Canada. In these olivines, the standard procedure of powdering grains to <30 µm failed to effectively remove mantle helium prior to fusion: samples from four different flows yielded unusually high powder fusion ^{4}He concentrations of 40 to 141 ncc/g with ^{3}He/^{4}He ratios of 7.9 to 9.6 R_A. When combined with the ^{3}He/^{4}He ratios obtained by crushing (average 8.1 ± 0.2 R_A), these measurements yield Holocene cosmogenic exposure ages but with very large uncertainties arising from the large mantle ^{3}He correction. The inability to effectively isolate ^{3}He$_c$ from these samples likely arises from the survival of small (<<30 µm) fluid inclusions hosting mantle He through the powdering step. The presence of such unusually small fluid inclusions may relate to the origin of the olivines as disaggregated peridotite xenoliths rather than the more commonly analyzed olivine phenocrysts. We circumvented this problem by step-heating powdered olivine in steps of 800, 1000, and 1400ºC. Helium isotopic systematics indicate that 70-90 % of ^{3}He$_c$ was released in the low temperature step and the rest was released in the middle temperature step. By the highest temperature step, the released He had a mantle-like ^{3}He/^{4}He ratio. Combining results from the step heating and crush-fusion methods, we determined that the four Volcano Mountain lava flows erupted approximately coevally, at 10.5 ± 1.7 ka.

1 Introduction

The in-situ production of cosmogenic ^{3}He in olivine has been used to date the surface exposures of lava flows for decades (e.g. Aciego et al., 2007; Kurz et al., 1990; Marchetti et al., 2020). The abundance of mm-size olivine crystals in basalt and the high helium retentivity of olivine (Shuster and Farley, 2004; Trull and Kurz, 1993) make it an ideal candidate for cosmogenic ^{3}He dating. The method is particularly suited to the determination of eruption ages of young volcanics (Heineke et al., 2016; Fenton and Niedermann, 2014; Licciardi et al., 1999) because ^{3}He has one of the highest production/detection limit ratios amongst cosmogenic nuclides (Niedermann, 2002).

Deleted:
Deleted: very
Deleted: s
Deleted: Yukon, Canada
Deleted: .
Deleted: adequately
Deleted:
Deleted: analyses
Formatted: Superscript
Formatted: Superscript
Formatted: Subscript
Deleted: . For example, in one powder fusion the concentration of ^{4}He was 109 ncc STP/g with a ^{3}He/^{4}He ratio of 8.7 ± 0.3 R_A. Based on the ^{3}He/^{4}He ratio of 8.1 ± 0.2 R_A released by crushing of the same sample, the estimated fraction of mantle ^{3}He in the powder fusion is between 87 % and 98 % of the total ^{3}He.
Formatted: Superscript
Deleted: Regardless, the high proportion of mantle ^{3}He in the powder fusion yields highly uncertain ^{3}He$_c$ exposure ages.
Deleted: a three-step heating schedule ranging from 700 to 1400°C…
Deleted: 80-92
Formatted: Superscript
Deleted: Using this technique on two samples from the youngest VM flow, we obtained precise estimates of cosmogenic ^{3}He concentrations, from which we derive an eruption age of 10.9 ka ± 1.1 ka. …¶
¶
Deleted: ¶
Deleted: e the
Deleted: exposure

Cosmogenic ^3He in terrestrial rocks is primarily produced by spallation of target nuclei in the crystal lattice of minerals. At surface temperatures, ^3He_c accumulates quantitatively in the matrix of olivine (Kurz, 1986a, 1986b), allowing exposure ages to be obtained from independently established production rates. Unlike cosmogenic radionuclides such as ^{10}Be and ^{26}Al in which the background nuclide concentration is often negligible, a practical challenge of the ^3He method is isolating the cosmogenic component from other ^3He components. The most common non-cosmogenic sources of ^3He include thermal neutron capture on ^6Li (Andrews and Kay, 1982; nucleogenic ^3He, $^3He_{nuc}$) and mantle He with $^3He/^4He$ ratios well above crustal values trapped in fluid inclusions (Kurz, 1986a, 1986b). U and Th-bearing minerals also produce radiogenic ^4He ($^4He_{rad}$) through α decay. Taken together:

$$^3He_{total} = {}^3He_c + {}^3He_m + {}^3He_{nuc} \quad (1)$$

$$^4He_{total} = {}^4He_m + {}^4He_{rad} \quad (2)$$

However, concentrations of Li, U, and Th in olivine tend to be low (Woodhead, 1996; Dostal and Capedri, 1975; Kent and Rossman, 2002; Blard and Farley, 2008; Amidon et al., 2009; Blard et al., 2013) such that neutron capture and radioactive decay produces minimal amounts of He in most young lava flows. Thus, in the specific limiting case in which nucleogenic/radiogenic He can be ignored:

$$^3He_{total} = {}^3He_c + {}^3He_m \quad (3)$$

$$^4He_{total} = {}^4He_m \quad (4)$$

Equation 3 highlights that cosmogenic ^3He dating in young olivine requires the isolation of ^3He_c from ^3He_m. Past studies (e.g., Kurz, 1986a) achieved sufficient separation of the two components using a two-step process in which the first step is crushing whole olivine grains in vacuum and measuring the $^3He/^4He$ ratio. Vacuum-crushing olivine grains to <500 µm releases most mantle He in fluid inclusions and yields the crush ratio for a given sample, $(^3He/^4He)_{crush}$ (Kurz, 1986a, 1986b; Puchol et al., 2017; Blard, 2021). In the second step, the crushate is powdered to reduce the number of surviving fluid inclusions, and then fused in vacuum to measure mostly matrix-hosted He. In basalts, crush ratios are often close to the upper mantle ratio of ~8 times the atmospheric ratio ($R_A = 1.384 \times 10^{-6}$), while fusion ratios ($(^3He/^4He)_{fusion}$) of cosmic-ray irradiated samples may be several times higher (Kurz, 1986a, 1986b). If $^4He_{fusion}$ is assumed to be entirely mantle derived (eq. 4), then the cosmogenic component can be isolated even if some of the He in the fusion is mantle derived:

$$^3He_c = {}^3He_{fusion} - ({}^4He_{fusion})(^3He/^4He)_{crush} \quad (5)$$

^3He_c is then used to calculate an exposure age. The uncertainty on ^3He_c depends in part on how large and how well-known the correction for mantle He is. When powdering does not effectively remove the mantle component, the correction can be large compared to the total ^3He measurement.

Formatted: Indent: First line: 0"

Deleted: is

Deleted: eliminate any

Deleted:

Deleted: C

Deleted: $((^3He/^4He)_{crush})$

Deleted: in basalts

Deleted:)

Deleted: much

Deleted: An alternative way to estimate the cosmogenic component is to create a helium isochron (Blard, 2021; Blard and Pik, 2008 Cerling and Craig 1994). In this method, the crush step is skipped, and multiple aliquots (n) of a sample or samples with the same mantle component and exposure age are fused individually and used to create a helium isochron based on the following equation: ¶
$^3He^n_{total} = {}^3He_c + ({}^4He^n_m)(^3He/^4He)_m$ (6)¶
For n ≥ 2, this is a solvable system of equations with 2 unknowns (^3He_c, $(^3He/^4He)_m$). If the aliquots have sufficiently different ^4He concentrations, a line regressed through a plot of ^3He vs ^4He has can be used to estimatea slope of both $(^3He/^4He)_m$ and a y-intercept of ^3He_c (Blard, 2021). Equivalently, a plot of $^3He/^4He$ vs $1/^4He$ can be used in the same fashion(Cerling and Craig 1994). As with the crush-fusion method, the concentration of ^3He_c is used to calculate an exposure age and the uncertainty of this age rises as ^3He_m gets closer to the mantle ^3He component becomes a larger fraction of 3Hetotalthe total ^3He.

In this study, we attempted the crush-fusion method to obtain exposure ages for the youngest lava flows from Volcano Mountain in Yukon, Canada, however the mantle component was so large and well-retained during powdering that precise ^3He_c concentrations could not be obtained. As an alternative we applied a protocol previously used on cosmic-ray exposed peridotites (Swindle et al., 2023) in which step heating successfully isolated cosmogenic ^3He from mantle ^3He.

2 Geologic Setting

The Fort Selkirk Volcanic Complex in Yukon, Canada is comprised of valley-filling volcanics that interacted with Cordilleran ice sheets during the Pliocene and Pleistocene epochs (Jackson et al., 2012; Jackson and Huscroft 2023). Radiometric ages on the complex range from 0.4 to 4.3 Ma Jackson and Huscroft 2023. Volcano Mountain, also called Nelruna in the local First Nations language, is located north of the confluence of the Yukon and Pelly Rivers and is the youngest volcanic center in the complex (Jackson and Stevens, 1992). It rises several hundred meters above the valley fill and is comprised of lava flows, some of very youthful appearance. Among the more recent flows are several that dammed small lakes in the early-mid Holocene, some time before 7300-4200 BP (Jackson and Stevens, 1992; Francis & Ludden, 1990). The youngest flows could be even younger (Jackson and Stevens, 1992; Francis & Ludden, 1990). Jackson and Huscroft (2023) provide detailed field descriptions, photographs, and an eruptive history of Volcano Mountain.

Volcano Mountain lava flows are nephelinites carrying ultramafic xenoliths (mostly dunite) and olivine phenocrysts and xenocrysts (Francis & Ludden, 1990; Trupia & Nicholls, 1996). The xenocrysts are large (up to 1 cm) and are the dominant population of olivine crystals in the rock. Based on deformation features such as kink-banding and subgrain boundaries, their anhedral/broken shape, and highly magnesian composition (Fo88-90), they are likely disaggregated dunite xenoliths (Francis & Ludden, 1990; Trupia & Nicholls, 1996). These abundant and large xenocrysts are an attractive target for cosmogenic ^3He dating.

3. Samples

3.1 Field Sampling

Sampling of Volcano Mountain lavas was intended to date flows of the most youthful appearance and stratigraphic position to determine the age of the most recent eruption (Table 1; Fig.1). Particular attention was paid to the flow within the small summit crater as the most likely to be the youngest. For redundancy purposes, 2-3 samples were collected at each location. Site parameters used to guide sampling included: a relatively flat, stable surface exhibiting primary depositional features (e.g. ropy textures) and if possible, minimal vegetation cover. A gas-powered cutoff saw was used to control sampling by slicing the surface to a uniform depth. A rock hammer and chisel were used to liberate the sample from the prepared area. Approximately 2 kg of sample was collected from each site.

Deleted: both
Deleted: and the isochron method
Formatted: Indent: First line: 0"
Deleted: .
Deleted: .
Deleted: In both approaches
Deleted: developed
Deleted: step heating
Deleted: following work
Deleted: where
Deleted: samples
Deleted: partially
Deleted: c
Formatted: Highlight
Deleted: ,
Deleted: cone
Deleted: Volcano Mountain
Deleted: that
Deleted: . Radiocarbon ages of lake bottom sediments indicate that the lavas
Deleted: predate
Deleted: .
Deleted: m
Deleted: olivine phenocrysts,
Deleted: ,
Formatted: Indent: First line: 0"
Deleted: spinel lherzolite xenoliths
Deleted: Cosmogenic s
Deleted: the
Deleted: flows
Deleted: multiple
Formatted: Space After: 12 pt
Deleted: of the mountain
Deleted: date the last eruption
Deleted: then
Deleted: ¶
Deleted: (Fig.1)
Deleted: Notes collected included: location, average sample depth, distance from edges, surface slope angle and aspect, weathering characteristics (surface relief), vegetation cover, and topographic shielding.

A total of 13 samples were collected on six separate lava flow surfaces. Jackson and Stevens (1992) (see also Jackson and Huscroft 2023) mapped VM flows and named them based on the direction of the flow (north or south) and its stratigraphic position relative to the other flows based on field observations (0-2 where 2 is assigned to the youngest flows) (Fig. 1). Samples VM-01, 02, and 03 were collected from the stratigraphically highest flow in the cinder cone (flow 2Na). VM-06 is from the fifth south flow (flow 2Sa), VM-08 and 09 are samples from the third south flow (flow 1Sa) and VM-10 and VM-11 are samples from the second north flow (flow 1N). Samples VM-04, 05, 12, and 13 are from the fourth south flow (flow 2Sb, possibly the same age as flow 2Sa, Jackson and Huscroft 2023), but along with sample VM-07 (flow 2Sa), yielded too little olivine to make a cosmogenic ^{3}He measurement. See Table 1 for sample details.

At elevations ranging from ~0.7-1.1 km, the area experiences on average 28.8 cm of snow cover for 5.5 months of the year (Government of Canada, 2007). Vegetation, including lichen and moss, covered a significant surface area of the samples, though it is highly variable, from no coverage at VM-03 to covered in 8 cm thick mat of moss at VM-08.

Table 1

Flow	Sample	Latitude (N)	Longitude (W)	Elevation (m)	Depth (cm)	Shielding Factor
2Na	VM-01	62.92311	137.3775	1052	3	0.96
2Na	VM-02	62.92302	137.3779	1067	3	0.96
2Na	VM-03	62.92302	137.3779	1067	3.5	0.96
2Sa	VM-06	62.90544	137.43741	718	3	0.97
1Sa	VM-08	62.90447	137.4359	725	2.5	0.96
1Sa	VM-09	62.90413	137.43684	725	2	0.96
1N	VM-10	62.95478	137.36848	788	3.5	0.98
1N	VM-11	62.9547	137.36888	785	3.5	0.97

3.2 Sample Selection and Preparation

All hand samples were scrubbed of vegetation, rinsed in water, dried in air, and jaw-crushed to mm-sized grains. The abundance of coarse olivine crystals varied among samples; only samples VM-01, 02, 03, 06 and 08 through 11 had sufficient olivine for cosmogenic ^{3}He measurement. From these, matrix-free, mm-size olivine crystals were handpicked from the crushate based on their distinct lack of cleavage and green color.

Deleted: 6…separate lava flow surfaces.. ... [1]
Formatted: Highlight
Deleted: age …osition relative to the other flows based on field observations (0-2 where 2 is assigned to the youngestyoungest flows) (Fig. 1….. SS…mples VM-01, 02, and 03 were collected from the stratigraphically highestyoungest…flow in the cinder cone (flowFig. 1;…2Na). VM-06 and VM-07 sample…s from the fifth south flow (flow Fig. 1; …Sa),….VM-08 and 09 are samples from the third south flow which is the oldest flow based on field observations…(flow Fig. 1; …Sa) and.…VM-10 and VM-11 are samples from the second north flow (flow Fig. 1; ... [2]
Formatted ... [3]
Deleted:
Deleted: entirely …overed in 8 cm thick mat of moss at VM ... [4]
Formatted: Font color: Text 1
Deleted: ¶
Deleted:
Deleted: Table 1 Sample Information ... [5]
Deleted: and …insed in water, dried in air, and. Hand samples were…jaw-crushed to mm- ... [6]
Deleted: M…matrix-free, mm-size olivine crystals mm-sized olivine …ereas…handpicked from the crushate based on their distinct lack of cleavage and green color. ... [7]
Formatted: Superscript
Deleted: Table 1 Sample Information ... [8]

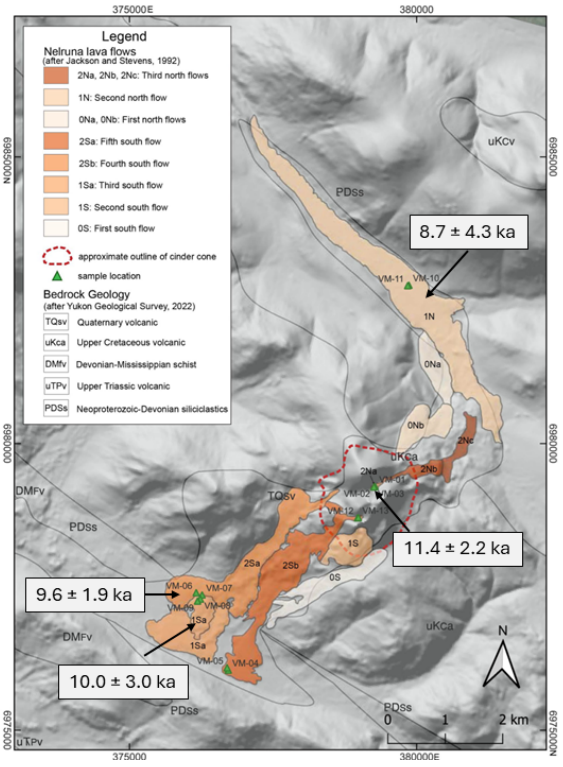

260 **Figure 1. Geologic Map of Volcano Mountain (Nelruna). Map of Volcano Mountain study area after Jackson and Stevens (1992).** Samples VM 01,02, and 03 are from the stratigraphically youngest flow on Volcano Mountain, while the other samples all come from flows of very youthful appearance. Numbers in boxes indicate our best estimate of eruption age based on cosmogenic ^{3}He.

265

Formatted: Centered

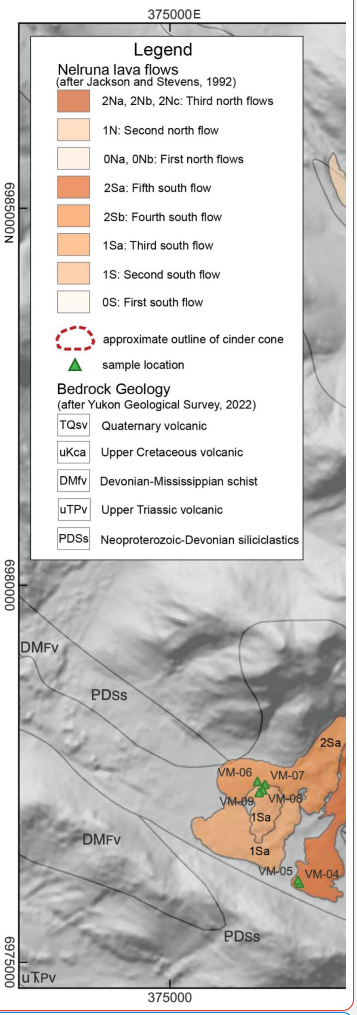

Deleted:

Formatted: Justified

4 Analytical Methods

4.1 Crushing and Powder Fusion Method

Helium was extracted from olivines by crushing under vacuum for 2 min, and then re-crushed for another 5 min. The two steps were combined into a single He result. Previous work with this same crusher design indicates these crush durations will not cause release of matrix-sited ^{3}He (Blard et al., 2008). Prior to dropping samples into the crusher anvil, 2 minute "no sample" crushes were measured and used to blank correct He measurements. Maximum blank crush levels of ^{3}He and ^{4}He were 0.07 fcc STP and 0.2 ncc STP, respectively.

For some samples, material recovered from the vacuum crushes was powdered in a mortar and pestle under ethanol and sieved to <30 µm, dried, weighed, and wrapped in Sn foil packets for fusion analysis. For other samples analyzed by fusion, the hand-picked olivines did not undergo the initial vacuum-crush step, only powdering under ethanol. Ethanol was used to circumvent (Cox et al., 2022) trapping of atmospheric He during powdering (Protin Blard and Mathon 2016).

Sn-foil wrapped samples for high temperature vacuum extraction analysis were loaded into the dropper arm of a double-wall furnace and evacuated overnight. The dropper arm was not heated to eliminate any possibility of baking-induced loss of ^{3}He. The furnace was outgassed directly into the vacuum pump for 1 hr at 1400°C prior to analysis. Samples were then dropped into a carbon liner in the furnace and heated to ~1200 °C for 25 min. Re-extracts were measured directly after each extraction to ensure the complete release of helium. When the re-extract signal exceeded the pre-analysis hot blank, the re-extract was repeated. All sample gas in excess of blank was combined in the concentrations reported here. While these olivines were not fused during these analyses (the temperature was held sub-melting to minimize He blanks), complete He extraction is ensured by the re-extraction steps. For consistency with prior work we nevertheless refer to these measurements as "powder fusions". Two olivine samples were fused in a lithium borate flux at ~1000 °C for 25 min in a molybdenum liner. The flux was used in these fusions to reduce blank He levels by lowering extraction temperature (Farley et al., 2020). Hot blanks at ~1200 °C for ^{3}He and ^{4}He were 0.8 fcc STP and 0.2 ncc STP respectively. Blanks measured on the tin foil are negligible compared to this hot furnace blank. Blank corrections made to sample gas concentrations were mostly <2% but always <5%.

4.2 Step-heating

About 750 mg of powdered (<30 µm) sample was wrapped in Sn foil packets and loaded into the vacuum furnace as described above. The Sn packets were then dropped into the furnace, and He successively released at 800 °C, 1000 °C, and 1400 °C each for 30 minutes duration. These temperature steps were selected based on previous studies reporting the release of cosmogenic

Deleted: **Figure 1. Geologic Map of Volcano Mountain (Nelruna)** Crush-fusion analyses were done using powdered olivine xenocrysts from VM-02, 06, 08, 09, 10, and 11. Powdered olivine from VM-01 and VM-03 was step-heated. 3Hec exposure ages are reported in Table 4.¶

¶

Deleted: -

Deleted: Handpicked o

Deleted: were crushed u

Deleted: following Blard et al. (2008).

Formatted: Superscript

Deleted: recovered

Deleted: from

Deleted: ¶

Deleted:

Deleted: (Cox et al., 2022).

Formatted: Highlight

^{3}He below 1000 °C (Kurz, 1986a; Swindle et al., 2023). A thermocouple and pyrometer were used to calibrate furnace temperatures as a function of furnace output power, after which heating steps were maintained using constant power output.

Hot blanks were performed on an empty furnace at each of the scheduled temperature steps to use as blank corrections on He quantities at each step. Blank levels were <1.5 % of extracted He for all steps. Re-extracts were measured on the material after step-heating to ensure total helium release. When the re-extract signal exceeded the pre-analysis hot blank, the re-extract was repeated. When the re-extract exceeded the hot blank, the excess He was added to the high temperature step.

4.3 Helium Measurement

Helium was purified and measured as previously described (Horton et al., 2019; Swindle et al., 2023). Gas extracted from the furnace was passed through a charcoal U-trap to remove contaminants such as CO_2, H_2O, and Ar. Remaining reactive gases were removed using a hot SAES NP10 getter and H_2 was removed using a cold SAES NP10 getter. Helium was then cryofocused on charcoal at 14 K and released at 34 K into a Helix SFT mass spectrometer. ^{3}He was measured on a pulse-counting electron multiplier and ^{4}He on a Faraday cup. Instrument sensitivity and internal consistency were monitored by running a standard containing ~70 ncc of He (^{3}He/^{4}He ratio = 2.05 R_A) throughout our experiments. This standard was created from pure ^{3}He and ^{4}He using a capacitance manometer and the amounts delivered are known to better than ±1 %.

4.4 Shielding Correction

Corrections for snow cover, vegetation cover, and self-shielding were considered for every sample. The snow correction factor was calculated using Eq. 3 in Vermeersch (2007) based on the spallogenic neutron attenuation length, average snow thickness, and snow density. A snow density of 0.3 g/cm^3 was assumed. Topographic shielding corrections were made for VM-01, 02, and 03 due to their location inside the VM cinder cone (see red outline in Fig. 1). Topographic shielding for the other samples was negligible. Shielding factors are listed in Table 1.

5 Results

5.1 Crush and Fusion Results

Analytical results for the crushing and fusion experiments are listed in Table 2. The three samples (VM-02, VM-06, and VM-09) analyzed by crushing come from three different flows (2Na, 2Sa, and 1Sa) yet have indistinguishable crush ^{3}He/^{4}He ratios (7.99 ± 0.19, 8.08 ± 0.19, and 8.23 ± 0.2 R_A). Crush-release He concentrations in these samples are high for basalt-hosted olivines, ranging from 76 to 184 ncc/g/

Deleted: ¶
¶

Deleted: Sn-foil wrapped samples for fusion high temperature vacuum extraction analysis were loaded into the dropper arm of a double- wall furnace and evacuated overnight. The dropper arm was not heated to eliminate any possibility of baking-induced loss of ^{3}He. The furnace was outgassed directly into the vacuum pump for 1 hr at 1400ºC prior to analysis. evacuated overnight without baking. Samples were then dropped into a carbon liner in the furnace and heated to ~1200 °C for 25 min. Re-extracts were measured directly after each extraction to ensure the complete release of helium. When the re-extract signal exceeded the pre-analysis hot blank, the re-extract was repeated. All sample gas in excess of blank was combined in the concentrations reported here. While these olivines were not fused during these analyses (the temperature was held sub-melting to minimize He blanks), complete He extraction is ensured by the re-extraction steps. For consistency with prior work we nevertheless refer to these measurements as "powder fusions". Two analyses olivine samples were fused with the help of in a lithium borate flux at ~1000 °C for 25 min in a molybdenum liner. The flux was used in these later fusions to reduce blank He levels by lowering extraction temperature (Farley et al., 2020). Hot blanks at ~1200 °C for the empty furnace were measured for powder fusions. Maximumfor hot blank levels of ^{3}He and ^{4}He were 0.8 fcc STP and 0.2 ncc STP respectively. Blanks measured on the tin foil are negligible compared to this hot furnace blank. Although bBlank levels corrections made to sample gas concentrations were are insignificant (mostly <2% but always <5 %) compared to levels of extracted helium, blank corrections were still made to all He measurements. . ¶
4.2 Step-heating¶
About 750 mg of powdered (<30 µm) sample was wrapped in Sn foil packets and loaded into the vacuum furnace as described above. that were then loaded into the dropper arm of a double walled furnace that was evacuated overnight without baking. The Sn packets were then dropped into the furnace, and He successively released at 800 °C, 1000 °C, and 1400 °C each for 30 minutes duration.at sequential low, middle, and high temperature steps. These Ttemperature steps were selected held for 30 min at 800 °C, 1000 °C, and 1400 °C were chosen for this experiment based on previous studies that observereporting the release of cosmoge ... [9]

Formatted: Indent: First line: 0"

Deleted: ¶

Deleted: E

Deleted: at 34 K

Deleted: was

Deleted: based

Deleted: on

Deleted: ¶

Formatted: Font: Not Bold

Formatted: Font: Not Bold

Formatted: Subscript

Deleted: Results are shown in Table 2. Early measurements focused on samples with the most abundant separable olivine. Vacuum crushing of VM-06 and VM-09 revealed a mantle ^{3} ... [10]

Six powder fusion analyses and the total helium yield from the three step heats (described below) provide information on the matrix-hosted helium in all four of the investigated lava flows. Across these nine analyses, He concentrations range from 39 to 141 ncc STP/g, similar to the crush results. $^{3}He/^{4}He$ ratios ranged from 7.9 ± 0.2 to 9.6 ± 0.2 R_A. For the three lava flows on which both crushing and fusion analyses are available, fusion $^{3}He/^{4}He$ ratios ranged from the same within error as the crush result (VM-09 from flow 1Sa), to a maximum of 1.5 R_A higher (VM-06 from flow 2Sa).

Table 2

Flow	Sample	Analysis Type	Mass g	^{3}He pcc/g	±	^{4}He ncc/g	±	$^{3}He/^{4}He$ R_A	±	$^{3}He_c$ Mat/g	±	$^{3}He_c$ %
2Na	VM-02	Crush	0.097	2.04	0.04	183.7	3.7	7.99	0.19			
2Na	VM-02	Fusion	0.246	1.31	0.03	109.0	2.2	8.67	0.25	2.75	1.25	7.8
2Na	VM-01	StepHt	0.734	1.13	0.04	91.0	3.2	8.96	0.26	3.27	1.57	10.8
2Na	VM-03	StepHt	0.800	1.32	0.05	104.9	3.7	9.03	0.25	4.05	1.82	11.4
2Sa	VM-06	Crush	0.630	0.85	0.02	75.6	0.9	8.08	0.19			
2Sa	VM-06	Fusion	0.500	0.51	0.01	38.6	0.8	9.59	0.27	2.19	0.36	15.8
1Sa	VM-09	Crush	0.100	1.22	0.02	106.5	1.4	8.23	0.20			
1Sa	VM-09	Fusion	0.068	0.51	0.04	46.1	1.8	7.94	0.71	-0.51	1.16	
1Sa	VM-08	Fusion	0.320	0.70	0.01	53.4	1.1	9.37	0.27	2.27	0.64	12.1
		Assumes average of all VM crushes:						8.10	0.20			
1N	VM-10	Fusion	0.116	0.55	0.04	47.4	1.0	8.36	0.33	0.46	1.17	3.1
1N	VM-11	Fusion	0.100	1.15	0.02	100.3	2.0	8.25	0.24	0.56	1.15	1.8
1N	VM-11	StepHt	0.657	1.65	0.06	140.6	4.9	8.44	0.41	1.79	2.37	4.0

We used these data to compute cosmogenic ^{3}He concentrations via equation 1 by assuming that the crush $^{3}He/^{4}He$ ratio on a given flow can be applied to all samples obtained from that flow. For flow 1N, for which we did not measure a sample by crushing, we computed cosmogenic ^{3}He concentrations by assuming the mean crush $^{3}He/^{4}He$ ratio of 8.1 ± 0.2 R_A obtained on the other flows. This assumption is supported by the step heat results described below.

Cosmogenic ^{3}He was confidently detected in five of the nine fusion analyses (Table 3). For flow 2Na we obtained cosmogenic ^{3}He concentrations of 2.75 ± 1.25 Mat/g (VM-02), 3.27 ± 1.57 Mat/g (VM-01), and 4.05 ± 1.82 Mat/g (VM-03). One analysis each of flow 2Sa (VM-06) and 1Sa (VM-08) yielded $^{3}He_c$ of 2.19 ± 0.36 and 2.27 ± 0.64 Mat/g, respectively. For the remaining

Formatted: Font: Not Bold
Formatted: Superscript
Formatted: Superscript
Formatted: Superscript
Formatted: Superscript
Formatted: Subscript
Formatted Table
Deleted: ¶
Deleted: ¶
Formatted: Superscript
Formatted: Superscript
Formatted: Superscript
Formatted: Superscript
Formatted: Superscript
Formatted: Superscript
Formatted: Subscript
Formatted: Superscript
Formatted: Superscript
Formatted: Superscript
Formatted: Subscript

four analyses the 1 sigma analytical uncertainty on ^3He_c exceeds the measured value, i.e., the cosmogenic ^3He concentration is indistinguishable from zero.

The high analytical uncertainties on ^3He_c - typically more than 1 Mat/g - in the VM samples arises from the large corrections required for mantle ^3He present in the powder fusion analyses (equation 1). For example, as shown in Table 2, the fraction of ^3He that is cosmogenic in these analyses ranges from a maximum of 15.8% (VM-06) to < 2% (VM-11, VM-09). Stated differently, the $^3He/^4He$ ratios obtained by fusion are very close to the ratios obtained by crushing, and this similarity at least in part reflects preservation of a high concentration of mantle helium through the powdering step.

Table 3

Flow	Sample	Mass g	Step ºC	^3He pcc/g	±	^4He ncc/g	±	$^3He/^4He$ R_A	±	^3He_c Mat/g	±	^3He_c %
2Na	VM-01	0.734	800	0.34	0.01	19.8	0.4	12.28	0.35	3.26	0.27	35.9
			1000	0.29	0.01	25.2	0.5	8.35	0.24	0.45	0.30	5.8
			1400	0.50	0.01	46.0	0.9	7.87	0.22			
			Total	1.13	0.04	91.0	3.2	8.96	0.44			
			Total Cosmogenic							**3.71**	**0.41**	
2Na	VM-03	0.800	800	0.27	0.01	14.8	0.3	13.14	0.37	2.76	0.21	37.9
			1000	0.25	0.01	20.1	0.4	9.00	0.26	0.62	0.25	9.3
			1400	0.79	0.02	70.0	1.4	8.17	0.23			
			Total	1.32	0.00	104.9	0.3	9.03	0.44			
			Total Cosmogenic							**3.38**	**0.33**	
1N	VM-10	0.657	800	0.39	0.01	27.6	0.6	10.18	0.29	2.47	0.35	23.5
			1000	0.51	0.01	43.9	0.9	8.38	0.24	0.97	0.52	7.0
			1400	0.75	0.01	69.0	1.4	7.79	0.22			
			Total	1.65	0.06	140.6	4.9	8.44	0.41			
			Total Cosmogenic							**3.43**	**0.63**	

5.2 Step-heat

Because the crush-fusion method was not especially successful in isolating the cosmogenic component, we attempted step heating on two samples from the stratigraphically youngest flow (2Na, samples VM-01 and VM-03) and one from the stratigraphically oldest flows (Flow 1N, sample VM-10). Results are shown in Table 3 and Fig 2. In all three samples the

Formatted: Superscript
Formatted: Subscript
Formatted: Superscript
Formatted: Superscript
Formatted: Subscript
Formatted: Superscript
Formatted: Superscript
Formatted: Superscript
Formatted: Superscript
Formatted: Font: Bold
Formatted Table
Deleted: Two crush and six powder fusion analyses of olivine xenocrysts from Volcano Mountain were measured in this study (Table 2). A large fraction of mantle He was obtained from all powder fusions, with ^4He concentrations that range from 39 ± 1 to 110 ± 2 ncc STP/g. $^3He/^4He$ ratios of fusions ranged from 7.9 to 9.6 ± 0.2 R_A, with most fusions having slightly higher ratios compared to those obtained by crushing. Given that the crush ratio of 8.1 ± 0.2 R_A is likely representative of all VM samples, there are six crush-fusion pairs that can be used to calculate ^3He_c concentrations using Eq. 5. The highest concentration of ^3He_c we measured was 0.1 ± 0.02 pcc/g in VM-08 while the lowest concentration was within error of zero in VM-09. The mean concentration is 0.05 ± 0.02 pcc/g.¶
¶
¶
Table 2 Crush-fusion Results¶
Analysis ... [11]
Deleted: ¶
The isochron method (Cerling and Craig 1994, Blard 2021) offers an alternative way to obtain the cosmogenic ^3He concentration that eliminates the need to isolate the mantle component by crushing. This approach requires¶
This same fusion data can be cast as an isochron provided multiple analyses of a lava flow or flows that we assume the flows havecarry the same cosmogenic ^3He concentration exposure age and the same mantle componentcomposition. The three fusion analyses of flow 2Na (VM-01, 02, 03) satisfy these requirements, but have very little spread in ^4He (from 91 to 109 ncc/g). (Note that we cannot combine these results with the lower elevation flows to get more spread because the flows will not share the same cosmogenic ^3He concentration even if they have the same exposure age). A York regression of these three analyses plotted according to equation 6 yields a cosmogenic ^3He concentration of 5 Mat/g but with a very large uncertainty of 20 Mat/g. Analyses of the six samples of the three lower-elevation lava flows have a much larger spread in ^4He (39 to 141 ncc/g). If we assume these samples meet the isoc ... [12]
Deleted: Regression of the ^3He (pcc/g) and ^4He (ncc/g) concentration data from our VM fusions reveals a $(^3He/^4He)_m$ ratio of 8.1 ± 0.3 R_A (Fig. 3), which is consistent with our crush a ... [13]
Deleted: 3
Deleted: R
Deleted: 3 below

$^3He/^4He$ ratios decline monotonically with extraction temperature, while the ^4He yields increase. For example, in sample VM-03, the 800, 1000, and 1400°C steps yielded $^3He/^4He$ ratios of 13.1, 9.0, and 8.2 R_A, and ^4He concentrations of 15, 20, and 70 ncc/g, respectively. Previous work indicates that mantle He in fluid inclusions is released at extraction temperatures >1000°C (Swindle + other refs). In the case of the VM samples, the $^3He/^4He$ ratios extracted in the final steps (7.87 ± 0.22, 8.17 ± 0.23, 7.79 ± 0.22 R_A) are indistinguishable from the mean $^3He/^4He$ ratio obtained by crushing (8.10 ± 0.20 R_A), supporting this conclusion.

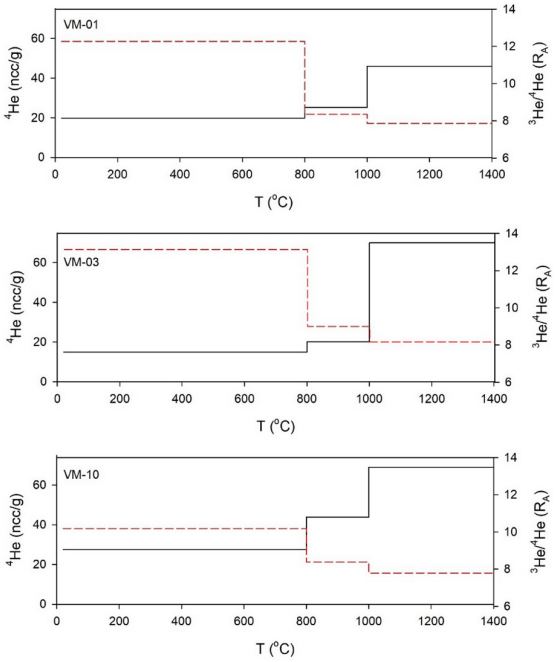

Figure 2. Step heat results on three of the VM samples. Samples were analyzed at three successive temperatures (800, 1000, 1400 °C) held for one half hour each. Horizontal lines indicate the temperature range over which each measurement integrates. Red dashed line indicates $^3He/^4He$ ratio (right hand axis) while black solid line indicates ^4He concentration (left hand axis).

Formatted: Superscript
Formatted: Superscript
Formatted: Superscript
Formatted: Superscript
Formatted: Subscript
Formatted: Superscript
Formatted: Superscript
Formatted: Highlight
Formatted: Subscript
Formatted: Subscript
Deleted: The low, middle, and high temperature steps of the VM-01 experiment yielded $^3He/^4He$ ratios of 12.3 ± 0.2, 8.3 ± 0.2, and 7.9 ± 0.2 R_A respectively. A similar trend is observed in the VM-03 step-heat experiment where the $^3He/^4He$ ratio evolved from 13.1 ± 0.2 to 9.0 ± 0.2, and then to 8.2 ± 0.2 R_A in the low, middle, and high temperature steps respectively. 92 % of the total ^3He_C was released during the low temperature step in VM-01 and 80 % was released in the low temperature step in VM-03. Mantle ^3He shows an opposite trend, with most mantle He released in the high temperature step in both step-heat experiments. ¶
Table 3 Step Heat Results¶
Sample ... [14]
Formatted: Highlight
Formatted: Centered
Formatted: Space Before: 0 pt, After: 0 pt
Formatted: Font: (Default) Times New Roman, Not Bold, Font color: Auto, Pattern: Clear

6 Discussion

6.1. Tightly Retained Mantle He in Volcano Mountain Olivine

$^3He/^4He$ ratios of He released by crushing and in the highest temperature step of the step heats are within the typical range of mid-ocean ridge basalts (Graham et al., 1992), suggesting He in Volcano Mountain derives from the upper mantle. Regardless of its origin, the presence of this mantle He substantially complicates determination of cosmogenic ^3He exposure ages. While mantle ^4He concentrations of crushed olivines are sometimes, but not often (Kurz et al., 1990; Farley and Neroda, 1998; Fenton and Niedermann, 2014; Heineke et al., 2016), as high as the ~100 ncc STP /g we obtained on the VM samples, the more important complication arises from the fact that this mantle He is not effectively removed by powdering to <30 um. Our powder fusion analyses indicate that about a third of the mantle component remains in the powdered olivine in every case. Our results suggest a mantle component that survives the powdering step, most likely in <<30 μm fluid inclusions. Evidence to support this interpretation cones from our observations of trails of circular voids (<10 μm) present in backscatter electron images of VM olivine xenocrysts. We interpret these to be secondary inclusion trails that carry mantle He. Survival of the mantle component when crushing this fine is not typical, but it is similar to results obtained on Twin Sisters peridotites (Swindle et al., 2023). Another possibility is that the ubiquitous kink banding and sub-grain boundaries observed in VM (Francis & Ludden, 1990) and Twin Sisters olivines (Swindle) could contribute to mantle He retention.

6.2 Component separation by step heating

The step-heat method takes advantage of the different release kinetics of matrix-sited and fluid inclusion-sited He. Diffusion alone is adequate to release matrix-sited helium; in contrast, for fluid inclusion helium to escape the crystal requires it to first dissolve into the olivine, an energetically disfavored process (Trull and Kurz 1993). Three temperature steps allowed us to be flexible about the temperature that best separates these two components. The evolution of the $^3He/^4He$ ratio with temperature thus can reveal two-endmember mixing between mantle and cosmogenic He (assuming radiogenic and nucleogenic helium are both absent).

Compared to the $^3He/^4He$ ratios obtained on powder fusions, the $^3He/^4He$ ratios of the lowest temperature steps in our step-heat experiments are between 1.5 and 4 R_A higher (Tables 2, 3). In contrast, $^3He/^4He$ ratios of the 1000°C steps are very similar to the powder fusion values, and about 0.7 R_A higher than the highest temperature steps and the associated crush-released $^3He/^4He$ ratios. These data provide support for the interpretation that all cosmogenic He is released prior to the highest temperature step, while mantle He is released in progressively greater amounts as step temperature increases.

To calculate the cosmogenic ^3He concentration from the step heat results for each sample, we assumed the final step represents the mantle component, used equation 1 to compute the cosmogenic ^3He yield in the two lower temperature steps, and combined

Deleted: ¶
¶
¶
¶
¶
¶
|↩|

Figure 3. Evolution of $^3He/^4He$ (circle), ^3He_c (solid line) and ^3He_m (dashed line) for VM-01 (red) and VM-03 (black) at the low, middle, and high temperature steps. By the high-T step, all ^3He_c has been released. Most ^3He_m is released in the high-T step, highlighting how much mantle He is retained in VM olivine xenocrysts.¶

Deleted: Our crush-released

Deleted: are within…are within the typical range of mid-ocean ridge basalts (Graham et al., 1992), suggesting He in Volcano Mountain derives from the upper mantle. Regardless of its origin, the presence of this mantle He substantially complicates our cosmogenic ^3He measurement ... [15]

Formatted: Space Before: 0 pt, After: 0 pt, Tab stops: Not at 0.36"

Formatted: Superscript

Deleted: ,…as high as the ~100 ncc STP /g we obtained from VM-09 (Table 2)…on the VM samples, (Kurz et al., 1990; Farley and Neroda, 1998; Fenton and Niedermann, 2014; Heineke et al., 2016), the greater …ore important complication arises from the fact that this mantle He is not effectively removed by powdering to <30 um. Our powder fusion analyses indicate that about . This is especially evident in samples VM-02 and VM-11, which have ^4He powder fusion concentrations as high as obtained by crushing … third of the mantle component remains in the powdered olivine in every case(Table 2)…¶
→Powder fusions of VM-09, 10, and 11 have $^3He/^4He$ ratios within error of the crush ratios. The remaining fusions are marginally better, with $^3He/^4He$ ratios ranging from 8.7 ± 0.2 to 9.6 ± 0.2 R_A (Table 2). The crush/fusion method relies on strong enrichment of the cosmogenic He component relative to the mantle component in the powder fusion. …Our results suggest a mantle component that survives the powdering step, most likely in <<30 μm fluid inclusions that remain intact until being melted during fusion… Evidence to support this interpretation cones fromare …our observations of trails of circular voids (<10 μm) present in backscatter electron images of VM olivine xenocrysts. We interpret theseThese ... [16]

Deleted: ¶

Formatted: Highlight

Formatted: Font: Not Bold, Font color: Auto, Pattern: Clear

Deleted: **High Degree of …omponent sS…paration in Low Temperature Step** ... [17]

Deleted: is based …akes advantage of the differenton the…release temperature …inetics of matrix-sited andvs…fluid inclusion-sited Diffusion alone is adequate to release matrix-sited helium; i ... [18]

Deleted: highest ···He/^4He ratios obtained from our datase ... [19]

Deleted: ~22-28 % higher.

Formatted: Subscript

Formatted ... [20]

them to obtain a total. Using this method, we obtained indistinguishable ^3He_c concentrations on the two samples of flow 2Na (3.71 ± 0.41 and 3.38 ± 0.33 Mat/g), and 3.43 ± 0.63 Mat/g on flow 1N. While still uncertain (average ± 13%), these cosmogenic concentrations are significantly better determined than by the crush/fusion method.

It is possible that a more detailed step heat could yield even greater degrees of separation between cosmogenic and mantle helium components, but at the potential cost of analytical precision associated with averaging multiple analyses and with blank corrections. Were significant amounts of radiogenic and/or nucleogenic helium present in these samples (unlikely given the eruption age of ~10 kyr, see below), this method would yield inaccurate results in the same way that the crush-fusion method would.

6.4 ^3He_c Exposure Ages

Exposure ages in Table 4 were computed from ^3He_c concentrations and corresponding uncertainties using the CRONUS-Earth online calculator (Balco et al., 2008; Phillips et al., 2016; version 3) where the production rate of ^3He_c is calibrated using data from Borchers et al. (2016). Exposure ages were obtained for four of the flows. By far the best determined is the exposure age of the youngest flow, 2Na. The two step heat analyses (VM-01, 03) yield indistinguishable ages of 12.3±1.9 and 11.1±1.6 ka. These are in good agreement with the three crush-fusion pairs (VM-01, 02, 03) with ages ranging from 9±4.2 to 13.3±6.1 ka. Assuming independent uncertainties among these analyses, the weighted means of these five ages is 11.4 ± 2.2 ka (MSWD 0.17, 95%), slightly more uncertain than the step heat analyses on their own. Four analyses were performed on flow 1N, with the step heat experiment yielding an age of 14.0±3.0 ka and three crush-fusion pairs yielding ages between 2.3±4.8 and 7.4±9.9 ka. The weighted mean of these analyses is 8.7 ± 4.3 ka (MSWD 2.3, 7.4%), again more uncertain than the step heat analysis by itself. The individual crush-fusion analyses of flows 2Sa and 1Sa yielded exposure ages of 9.6 ±1.9 ka and 10.0 ±3 ka, respectively.

Table 4

Flow	Sample	Method	^3He_c Mat/g	±	Exp Age ka	±
2Na	VM-01	C/F	2.75	1.25	9.0	4.2
	VM-02	C/F	3.27	1.57	10.8	5.3
	VM-03	C/F	4.05	1.82	13.3	6.1
	VM-01	StepHt	3.71	0.41	12.3	1.9
	VM-03	StepHt	3.38	0.33	11.1	1.6
	weighted mean				**11.4**	**2.2**
2Sa	VM-06	C/F	2.19	0.36	**9.6**	**1.9**

Formatted: Not Highlight

Formatted: Not Highlight

Deleted: and isochron

Deleted: s

Deleted: The percentage of cosmogenic 3He increases to 36-42 % when considering the lowest powder fusion $^3He/^4He$ ratio. The degree of separation (^3He_c /$^3He_{total}$) can also be used to evaluate the resolution between cosmogenic and mantle He. The highest degree of separation in crush/fusion analyses was ~16 %. In contrast, the degree of separation in the low temperature steps for VM-01 and VM-03 was 34 and 39 % respectively.

Formatted: Indent: First line: 0"

Deleted: In any case, the degree of separation obtained in these experiments provides a precise estimate of the exposure age of the VM flows.

Deleted: **6.3 Cross-Method Comparison of ^3He_c Concentrations**¶
In addition to the crush-fusion analyses and He isochron, the step-heating protocol was applied to VM-01 and VM-03. Like in the crush-fusion method, the measured ^4He and the ^3He /$^4He_{crush}$ ratio is used as a proxy for ^3He_m in each temperature step. The concentration of ^3He_c is calculated by subtracting the ^3He_m from $^3He_{total}$ for the low and middle temperature steps and then adding the cosmogenic components together:¶
$^3He_c = (^3He_{low\ temp} - (^3He/^4He_{crush})(^4He_{low\ temp})) + (^3He_{middle\ temp} - (^3He/^4He_{crush})(^4He_{middle\ temp}))$ (7)¶
The high temperature step was excluded because no ^3He_c was detected in this step. Equation 7 was used to calculate the cosmogenic ^3He concentration for the step-heat analyses, though it is worth noting that ^3He_c from the middle temperature step of VM-01 is negligible. ¶
The ^3He_c concentrations calculated using the crush-fusion, isochron, and step heat methods are listed in Table 4. Crush-fusion concentrations range from 0 to 2.58 ± 0.48 Matom/g ^3He_c and the mean is 1.33 ± 0.65 Matom/g for the 6 crush-fusion pairs. The He isochron method estimates a cosmogenic ^3He component of 1.34 ± 0.48 Matom/g and is within error of the crush-fusion mean. The step-heat method yielded the highest ^3He_c concentrations with the lowest uncertainties across methods (3.11 ± 0.28 and 3.50 ± 0.34 Matom/g).¶
¶
Table 4 ^3He_c
Concentrations¶
Method
... [21]

Deleted: (Table 5)

Formatted Table

1Sa	VM-08	C/F	2.27	0.64	**10.0**	**3.0**
1N	VM-10	C/F	0.46	1.17	1.9	4.8
	VM-11	C/F	0.56	1.15	2.3	4.8
	VM-11	C/F	1.79	2.37	7.4	9.9
	VM-10	StepHt	3.43	0.63	14.0	3.0
	weighted mean				**8.7**	**4.3**

Exposure ages are indicated on the map in Figure 1 using the weighted means when available. All four flows yield the same exposure age within error (weighted mean of all analyses: 10.5 ± 1.7 ka, MSWD 0.92, 51%) and there is no indication that the stratigraphically lower flows (1Sa and 1N, weighted mean 9.2 ± 3.5 ka, MSWD 1.8, 13%) have older exposure than the higher flows (2Na and 2Sa, weighted mean 11.0 ± 1.9 ka, MSWD .28, 93%).

The simplest interpretation of these results is that all of the studied VM lava flows erupted at 10.5 ±1.7 ka. Alternatively, honoring the stratigraphy the flows may have erupted over an age range from about 12.7 ka (1S flows) to about 9.1 ka (2Na and 2 Sa).

7 Conclusion

Volcano Mountain nephelinites contain olivine likely sourced from disaggregated peridotite xenoliths. This olivine contains high concentrations of upper mantle He and powdering does not effectively remove this component. Swindle et al. (2023) were similarly unable to remove mantle He components by powdering olivine from the Twin Sister peridotite. In both cases, this mantle He may be housed in fluid inclusions too small to be released by crushing. Alternatively, ubiquitous kink bands and subgrain boundaries seen in the Twin Sisters and Volcano Mountain flows could be the source of the He that survives powdering. In either case, survival of mantle He in VM powder fusions caused the crush-fusion method to yield imprecise ^3He_c concentrations. By using the step heating method described here, we were able to determine that the morphologically youngest lava flows on Volcano Mountain erupted approximately coevally in the earliest Holocene, 10.5 ±1.7 ka.

Data Availability

All data is provided in the figures and tables of this manuscript.

Author Contribution

Deleted: ¶

Deleted: Crush/fusion concentrations yield ^3He_c exposure ages ranging from 7.7 ± 4 ka to 11.1 ± 2.8 ka. Using the ^3He_c concentration from the He isochron (Fig. 3) and assuming an average elevation of 800 m and a shielding correction of 0.96, we calculate an exposure age of 5.2 ± 2.4 ka. In comparison, our step heat data yield ^3He_c exposure ages of 10.8 ± 1.3 ka and 11.1 ± 1.1 ka for VM-01 and VM-03 respectively. These ages are consistent with each other and have lower uncertainty than the exposure ages calculated using the crush-fusion or isochron ^3He_c concentrations. Since VM-01 and VM-03 are sampled from the same flow, we can average the ages to get 10.9 ± 1.1 ka. ¶

¶

Table 5 ^3He_c Exposure Ages¶

Analysis ... [22]

Deleted: and isochron

Deleted: s

Deleted: developed

Deleted: better isolate ^3He_c from ^3He_m, allowing us to obtain an exposure age for VM of 10.9 ± 1.1 ka.

J. M. Mueller prepared the manuscript with significant contributions from K. A. Farley and J. D. Bond. J. D. Bond and B.C Ward completed the field sampling.

Competing Interests

The authors declare that they have no conflict of interest.

Acknowledgements

We respectfully acknowledge and thank the Selkirk First Nation (SFN) for their support and guidance on this project. Roger Alfred and Elli Marcotte (SFN) provided traditional knowledge of Nelruna while in the field, which enlightened and guided our efforts. Sampling assistance was provided by Leyla Weston (YGS), Keyshawn Sawyer (SFN) and Sofia Bond (YGS). Funding for the field work was provided by the Yukon Geological Survey. Safe access to the area was provided by Malcolm Turnbull from Capital Helicopters. We would like to thank Dale and Sue Bradley from Pelly Ranch for their hospitality while completing the field work. This paper is assigned Yukon Geological Survey contribution number 066.

Deleted: ¶

References

Aciego, S. M., DePaolo, D. J., Kennedy, B. M., Lamb, M. P., Sims, K. W. W., and Dietrich, W. E.: Combining [He-3] cosmogenic dating with U-Th/He eruption ages using olivine in basalt, Earth And Planetary Science Letters, 254, 288–302, 2007.

Amidon, W. H., Rood, D. H., and Farley, K. A.: Cosmogenic He-3 and Ne-21 production rates calibrated against Be-10 in minerals from the Coso volcanic field, Earth and Planetary Science Letters, 280, 194–204, https://doi.org/10.1016/j.epsl.2009.01.031, 2009.

Andrews, J. N. and Kay, R. L. F.: Natural production of tritium in permeable rocks, Nature, 298, 361–363, 1982.

Balco, G., Stone, J. O., Lifton, N. A., and Dunai, T. J.: A complete and easily accessible means of calculating surface exposure ages or erosion rates from Be-10 and Al-26 measurements, Quaternary Geochronology, 3, 174–195, 2008.

Blard, P. H. and Pik, R.: An alternative isochron method for measuring cosmogenic 3He in lava flows, Chemical Geology, 251, 20–32, 2008.

Blard, P.-H.: Cosmogenic 3He in terrestrial rocks: A review, Chemical Geology, 586, 120543, https://doi.org/10.1016/j.chemgeo.2021.120543, 2021.

Blard, P.-H. and Farley, K. A.: The influence of radiogenic 4He on cosmogenic 3He determinations in volcanic olivine and pyroxene, Earth and Planetary Science Letters, 276, 20–29, https://doi.org/10.1016/j.epsl.2008.09.003, 2008.

Blard, P.-H., Braucher, R., Lavé, J., and Bourlès, D.: Cosmogenic 10Be production rate calibrated against 3He in the high Tropical Andes (3800–4900 m, 20–22° S), Earth and Planetary Science Letters, 382, 140–149, https://doi.org/10.1016/j.epsl.2013.09.010, 2013.

Cox, S. E., Miller, H. B. D., Hofmann, F., and Farley, K. A.: Short communication: Mechanism and prevention of irreversible trapping of atmospheric He during mineral crushing, Geochronology, 4, 551–560, https://doi.org/10.5194/gchron-4-551-2022, 2022.

Dostal, J. and Capedri, S.: Partition coefficients of uranium for some rock-forming minerals, Chemical Geology, 15, 285–294, https://doi.org/10.1016/0009-2541(75)90038-8, 1975.

Farley, K. A. and Neroda, E.: Noble gases in the Earth's mantle, Annu. Rev. Earth Planet. Sci., 26, 189–218, 1998.

Farley, K. A., Treffkorn, J., and Hamilton, D.: Isobar-free neon isotope measurements of flux-fused potential reference minerals on a Helix-MC-Plus mass spectrometer, Chemical Geology, 537, 119487, https://doi.org/10.1016/j.chemgeo.2020.119487, 2020.

Fenton, C. R. and Niedermann, S.: Surface exposure dating of young basalts (1–200 ka) in the San Francisco volcanic field (Arizona, USA) using cosmogenic 3He and 21Ne, Quaternary Geochronology, 19, 87–105, https://doi.org/10.1016/j.quageo.2012.10.003, 2014.

Graham, D. W., Jenkins, W. J., Schilling, J. G., Thompson, G., Kurz, M. D., and Humphris, S. E.: Helium isotope geochemistry of mid-ocean ridge basalts from the South Atlantic, Earth and Planetary Science Letters, 110, 133–148, 1992.

Heineke, C., Niedermann, S., Hetzel, R., and Akal, C.: Surface exposure dating of Holocene basalt flows and cinder cones in the Kula volcanic field (Western Turkey) using cosmogenic 3He and 10Be, Quaternary Geochronology, 34, 81–91, https://doi.org/10.1016/j.quageo.2016.04.004, 2016.

Horton, F., Farley, K., and Jackson, M.: Helium distributions in ocean island basalt olivines revealed by X-ray computed tomography and single-grain crushing experiments, Geochimica et Cosmochimica Acta, 244, 467–477, https://doi.org/10.1016/j.gca.2018.10.013, 2019.

Jackson, L. E. and Stevens, W.: A recent eruptive history of Volcano Mountain, Yukon Territory, https://doi.org/10.4095/132784, 1992.

Jackson, L. E., Nelson, F. E., Huscroft, C. A., Villeneuve, M., Barendregt, R. W., Storer, J. E., and Ward, B. C.: Pliocene and Pleistocene volcanic interaction with Cordilleran ice sheets, damming of the Yukon River and vertebrate Palaeontology, Fort Selkirk Volcanic Group, west-central Yukon, Canada, Quaternary International, 260, 3–20, https://doi.org/10.1016/j.quaint.2011.08.033, 2012.

Kent, A. J. R. and Rossman, G. R.: Hydrogen, lithium, and boron in mantle-derived olivine: The role of coupled substitutions, American Mineralogist, 87, 1432–1436, https://doi.org/10.2138/am-2002-1020, 2002.

Kurz, M. D.: Cosmogenic helium in a terrestrial igneous rock, Nature, 320, 435–439, 1986a.

Kurz, M. D.: In situ production of terrestrial cosmogenic helium and some applications to geochronology, Geochim Cosmochim Ac, 50, 2855–2862, 1986b.

Kurz, M. D., Colodner, D., Trull, T. W., Moore, R. B., and Obrien, K.: Cosmic-ray exposure dating with in-situ produced cosmogenic ^{3}He results from young Hawaiian lava flows, Earth Planet Sc Lett, 97, 177–189, 1990.

Licciardi, J., Kurz, M. D., Clark, P., and Brook, E.: Calibration of cosmogenic ^{3}He production rates from Holocene lava flows in Oregon, USA, and effects of the Earth's magnetic field, Earth Planet Sc Lett, 172, 261–271, 1999.

Marchetti, D. W., Stork, A. L., Solomon, D. K., Cerling, T. E., and Mace, W.: Cosmogenic 3He exposure ages of basaltic flows from Miller Knoll, Panguitch Lake, Utah: Using the alternative isochron approach to overcome low-gas crushes, Quaternary Geochronology, 55, 101035, https://doi.org/10.1016/j.quageo.2019.101035, 2020.

Niedermann, S.: Cosmic-ray-produced noble gases in terrestrial rocks: Dating tools for surface processes, in: Noble gases in geochemistry and cosmochemistry, vol. 47, edited by: Porcelli, D., Ballentine, C. J., and Wieler, R., Mineralogical Society of America, Washington D.C., 844, 2002.

Phillips, F. M., Argento, D. C., Balco, G., Caffee, M. W., Clem, J., Dunai, T. J., Finkel, R., Goehring, B., Gosse, J. C., Hudson, A. M., Jull, A. J. T., Kelly, M. A., Kurz, M., Lal, D., Lifton, N., Marrero, S. M., Nishiizumi, K., Reedy, R. C., Schaefer, J., Stone, J. O. H., Swanson, T., and Zreda, M. G.: The CRONUS-Earth Project: A synthesis, Quaternary Geochronology, 31, 119–154, https://doi.org/10.1016/j.quageo.2015.09.006, 2016.

Puchol, N., Blard, P.-H., Pik, R., Tibari, B., and Lavé, J.: Variability of magmatic and cosmogenic 3 He in Ethiopian river sands of detrital pyroxenes: Impact on denudation rate determinations, Chemical Geology, 448, 13–25, https://doi.org/10.1016/j.chemgeo.2016.10.033, 2017.

Shuster, D. L. and Farley, K. A.: 4He/3He thermochronometry, Earth and Planetary Science Letters, 217, 1–17, https://doi.org/10.1016/S0012-821X(03)00595-8, 2004.

Swindle, C., Clark, D., and Farley, K. A.: Helium isotope evidence for mixing of mantle-derived fluids and deeply penetrating surface waters in an obducted peridotite massif, Geochimica et Cosmochimica Acta, 353, 45–60, https://doi.org/10.1016/j.gca.2023.05.015, 2023.

Trull, T. W. and Kurz, M. D.: Experimental measurements of 3He and 4He mobility in olivine and clinopyroxene at magmatic temperatures, Geochimica et Cosmochimica Acta, 57, 1313–1324, https://doi.org/10.1016/0016-7037(93)90068-8, 1993.

Trupia, S. and Nicholls, J.: Petrology of Recent lava flows, Volcano Mountain, Yukon Territory, Canada, Lithos, 37, 61–78, https://doi.org/10.1016/0024-4937(95)00024-0, 1996.

Woodhead, J. D.: Extreme HIMU in an oceanic setting: the geochemistry of Mangaia Island (Polynesia), and temporal evolution of the Cook—Austral hotspot, Journal of Volcanology and Geothermal Research, 72, 1–19, https://doi.org/10.1016/0377-0273(96)00002-9, 1996.

Page 4: [1] Deleted	Farley, Kenneth A. (Ken)	1/1/25 3:16:00 PM

Page 4: [1] Deleted	Farley, Kenneth A. (Ken)	1/1/25 3:16:00 PM

Page 4: [2] Deleted	Farley, Kenneth A. (Ken)	11/5/24 12:37:00 PM

Page 4: [2] Deleted	Farley, Kenneth A. (Ken)	11/5/24 12:37:00 PM

Page 4: [2] Deleted	Farley, Kenneth A. (Ken)	11/5/24 12:37:00 PM

Page 4: [2] Deleted	Farley, Kenneth A. (Ken)	11/5/24 12:37:00 PM

Page 4: [2] Deleted	Farley, Kenneth A. (Ken)	11/5/24 12:37:00 PM

Page 4: [2] Deleted	Farley, Kenneth A. (Ken)	11/5/24 12:37:00 PM

Page 4: [2] Deleted	Farley, Kenneth A. (Ken)	11/5/24 12:37:00 PM

Page 4: [2] Deleted	Farley, Kenneth A. (Ken)	11/5/24 12:37:00 PM

Page 4: [2] Deleted	Farley, Kenneth A. (Ken)	11/5/24 12:37:00 PM

Page 4: [2] Deleted	Farley, Kenneth A. (Ken)	11/5/24 12:37:00 PM

Page 4: [2] Deleted **Farley, Kenneth A. (Ken)** **11/5/24 12:37:00 PM**

Page 4: [2] Deleted **Farley, Kenneth A. (Ken)** **11/5/24 12:37:00 PM**

Page 4: [2] Deleted **Farley, Kenneth A. (Ken)** **11/5/24 12:37:00 PM**

Page 4: [3] Formatted **Farley, Kenneth A. (Ken)** **1/2/25 8:34:00 AM**

Highlight

Page 4: [3] Formatted **Farley, Kenneth A. (Ken)** **1/2/25 8:34:00 AM**

Highlight

Page 4: [4] Deleted **Farley, Kenneth A. (Ken)** **11/7/24 11:31:00 AM**

Page 4: [4] Deleted **Farley, Kenneth A. (Ken)** **11/7/24 11:31:00 AM**

Page 4: [5] Deleted **Farley, Kenneth A. (Ken)** **12/20/24 10:16:00 AM**

Page 4: [6] Deleted **Farley, Kenneth A. (Ken)** **11/5/24 12:44:00 PM**

Page 4: [6] Deleted **Farley, Kenneth A. (Ken)** **11/5/24 12:44:00 PM**

Page 4: [6] Deleted **Farley, Kenneth A. (Ken)** **11/5/24 12:44:00 PM**

Page 4: [7] Deleted **Farley, Kenneth A. (Ken)** **11/5/24 12:43:00 PM**

Page 4: [7] Deleted **Farley, Kenneth A. (Ken)** **11/5/24 12:43:00 PM**

Page 4: [7] Deleted	Farley, Kenneth A. (Ken)	11/5/24 12:43:00 PM
Page 4: [7] Deleted	Farley, Kenneth A. (Ken)	11/5/24 12:43:00 PM
Page 4: [8] Deleted	Farley, Kenneth A. (Ken)	12/20/24 9:55:00 AM
Page 7: [9] Deleted	Mueller, Jessica M.	1/30/25 10:09:00 PM
Page 7: [10] Deleted	Farley, Kenneth A. (Ken)	11/5/24 2:41:00 PM
Page 9: [11] Deleted	Farley, Kenneth A. (Ken)	11/5/24 2:57:00 PM
Page 9: [12] Deleted	Mueller, Jessica M.	1/29/25 10:01:00 PM
Page 9: [13] Deleted	Farley, Kenneth A. (Ken)	12/21/24 3:58:00 PM
Page 10: [14] Deleted	Farley, Kenneth A. (Ken)	12/21/24 5:46:00 PM
Page 11: [15] Deleted	Farley, Kenneth A. (Ken)	1/2/25 8:44:00 AM
Page 11: [15] Deleted	Farley, Kenneth A. (Ken)	1/2/25 8:44:00 AM
Page 11: [16] Deleted	Farley, Kenneth A. (Ken)	1/2/25 2:38:00 PM
Page 11: [16] Deleted	Farley, Kenneth A. (Ken)	1/2/25 2:38:00 PM
Page 11: [16] Deleted	Farley, Kenneth A. (Ken)	1/2/25 2:38:00 PM
Page 11: [16] Deleted	Farley, Kenneth A. (Ken)	1/2/25 2:38:00 PM
Page 11: [16] Deleted	Farley, Kenneth A. (Ken)	1/2/25 2:38:00 PM

Page 11: [16] Deleted	Farley, Kenneth A. (Ken)	1/2/25 2:38:00 PM

Page 11: [16] Deleted	Farley, Kenneth A. (Ken)	1/2/25 2:38:00 PM

Page 11: [16] Deleted	Farley, Kenneth A. (Ken)	1/2/25 2:38:00 PM

Page 11: [16] Deleted	Farley, Kenneth A. (Ken)	1/2/25 2:38:00 PM

Page 11: [16] Deleted	Farley, Kenneth A. (Ken)	1/2/25 2:38:00 PM

Page 11: [16] Deleted	Farley, Kenneth A. (Ken)	1/2/25 2:38:00 PM

Page 11: [16] Deleted	Farley, Kenneth A. (Ken)	1/2/25 2:38:00 PM

Page 11: [16] Deleted	Farley, Kenneth A. (Ken)	1/2/25 2:38:00 PM

Page 11: [16] Deleted	Farley, Kenneth A. (Ken)	1/2/25 2:38:00 PM

Page 11: [16] Deleted	Farley, Kenneth A. (Ken)	1/2/25 2:38:00 PM

Page 11: [16] Deleted	Farley, Kenneth A. (Ken)	1/2/25 2:38:00 PM

Page 11: [16] Deleted	Farley, Kenneth A. (Ken)	1/2/25 2:38:00 PM

Page 11: [17] Deleted	Farley, Kenneth A. (Ken)	12/21/24 6:04:00 PM

Page 11: [17] Deleted	Farley, Kenneth A. (Ken)	12/21/24 6:04:00 PM

Page 11: [17] Deleted	Farley, Kenneth A. (Ken)	12/21/24 6:04:00 PM

Page 11: [18] Deleted	Farley, Kenneth A. (Ken)	1/1/25 6:13:00 PM

Page 11: [18] Deleted	Farley, Kenneth A. (Ken)	1/1/25 6:13:00 PM

Page 11: [18] Deleted	Farley, Kenneth A. (Ken)	1/1/25 6:13:00 PM

Page 11: [18] Deleted	Farley, Kenneth A. (Ken)	1/1/25 6:13:00 PM

Page 11: [18] Deleted	Farley, Kenneth A. (Ken)	1/1/25 6:13:00 PM

Page 11: [18] Deleted	Farley, Kenneth A. (Ken)	1/1/25 6:13:00 PM

Page 11: [18] Deleted	Farley, Kenneth A. (Ken)	1/1/25 6:13:00 PM

Page 11: [18] Deleted	Farley, Kenneth A. (Ken)	1/1/25 6:13:00 PM

Page 11: [19] Deleted	Farley, Kenneth A. (Ken)	1/2/25 8:53:00 AM

Page 11: [19] Deleted	Farley, Kenneth A. (Ken)	1/2/25 8:53:00 AM

Page 11: [20] Formatted	Farley, Kenneth A. (Ken)	1/2/25 9:01:00 AM

Superscript

Page 11: [20] Formatted	Farley, Kenneth A. (Ken)	1/2/25 9:01:00 AM

Superscript

Page 11: [20] Formatted	Farley, Kenneth A. (Ken)	1/2/25 9:01:00 AM

Superscript

Page 11: [20] Formatted **Farley, Kenneth A. (Ken)** **1/2/25 9:01:00 AM**

Superscript

Page 11: [20] Formatted **Farley, Kenneth A. (Ken)** **1/2/25 9:01:00 AM**

Superscript

Page 11: [20] Formatted **Farley, Kenneth A. (Ken)** **1/2/25 9:01:00 AM**

Superscript

Page 12: [21] Deleted **Farley, Kenneth A. (Ken)** **1/2/25 9:30:00 AM**

Page 13: [22] Deleted **Farley, Kenneth A. (Ken)** **1/2/25 10:49:00 AM**